Stephen Coss[1,2*] , Michael T Durand[1,2] , C.K. Shum[1,2] , Yuchan Yi[1], Xiao Yang[3], Tamlin Pavelsky[3], Augusto Getirana[4,5], Dai Yamazaki[6]

[1]Ohio State University, Columbus, OH

[2]Byrd Polar and Climate Research Center, Columbus, OH

[3]University of North Carolina at Chapel Hill, Chapel Hill, NC

[4] Hydrological Sciences Laboratory, NASA Goddard Space Flight Center, Greenbelt, MD

[5]Science Applications International Corporation, Greenbelt, MD, United States

[6]Institute of Industrial Science, The University of Tokyo, Meguro-ku, Tokyo, Japan

Corresponding author: Stephen Coss (coss.31@osu.edu)

Key Points:

- We introduce a 26-year record of entirely remotely sensed volumetric channel water storage anomaly.
- Storage climatology amplitude represents (0.04-12.54%) terrestrial water storage variability but just 0.2% of basin area.
- This new quantity can be used to analyze river spatial storage patterns in a way that was previously impossible.

Abstract

River channels store large volumes of water globally, critically impacting ecological and biogeochemical processes. Despite the importance of river channel storage, there is not yet an observational constraint on this quantity. We introduce a 26-year record of entirely remotely sensed volumetric channel water storage (CWS) change on 26 major world rivers. We find mainstem volumetric CWS climatology amplitude (CA) represents an appreciable amount of basin-wide terrestrial water storage variability (median 2.78%, range 0.04-12.54% across world rivers), despite mainstem rivers themselves represent an average of just 0.2% of basin area. We find that two global river routing schemes coupled with land surface models reasonably approximate CA (within ±50%) in only 11.5 % (CaMa-Flood) and 30.7 % (HyMap) of rivers considered. These findings demonstrate volumetric CWS is a useful quantity for assessing global hydrological model performance, and for advancing understanding of spatial patterns in global hydrology.

Plain Language Summary

Rivers are a critical part of global hydrology, but until now the variation in how much water rivers store has not been observed directly on the global scale. We created a 26 year record of this quantity across 26 of the world's largest rivers. We found that the storage variation in river main channels can represent up

to 12.54% of the total water variation estimates in a river basin despite only representing 0.2% of the total surface area. We also find that current methods to estimate this quantity through modeling (global river routing schemes coupled with land surface models) are only representing this quantity within 50% of our estimated value on between 11.5 % (CaMa-Flood) and 30.7 % (HyMap) of the rivers we studied. This demonstrates that this new quantity has value in assessing model performance and advancing the way we think about how rivers function as water storage vessels.

1 Introduction

While spaceborne sensors have revolutionized our understanding of global hydrology, some terms in the global water cycle remain poorly observed (Lettenmaier et al., 2015). Spaceborne sensors provide information about global processes that cannot be achieved with in situ measurements alone (Famiglietti et al., 2015). Despite their scientific potential, remote sensing measurements are thus subject to important limitations. For example, the Gravity Recovery And Climate Experiment (GRACE; Tapley et al., 2004, 2019) and GRACE Follow-On satellite missions have provided invaluable estimates of global water storage variability (Rodell et al., 2018) by estimating the total terrestrial water storage (TWS) anomaly, but do not provide information on individual hydrologic storage components such as soil moisture, snow, ground and surface water.

Surface water storage (SWS) in natural and artificial reservoirs, floodplains, wetlands and river channels is critical to human society and ecosystems, but complete compartmentalization of surface water storage from remote sensing measurements has remained elusive (Döll et al., 2012; Oki & Kanae, 2006). Estimates of the magnitude of SWS compared to total storage have been derived from global hydrologic models but vary widely: between 0 and 70% in Kim et al. (2009) as compared with a maximum of 27% from Getirana et al. (2017). Techniques to estimate SWS by subtracting other storage terms from GRACE TWS (e.g., Llovel et al., 2010; Swenson et al., 2008; Syed et al., 2008) are challenging because current estimates suggest that SWS contributes <10% of overall TWS variability on average (Getirana et al., 2017). Remote sensing estimates have shed light on storage change in major world floodplains (Papa et al., 2013; 2015), and on storage in global lakes and reservoirs (Gao et al., 2012; Tortini et al., 2020), but a comprehensive, observation-based quantification of storage change in rivers has not been previously presented. Storage change in rivers can be estimated directly from width and surface height measurements and can improve our understanding of global hydrologic model accuracy, and of the global water cycle.

The global estimates of river storage presented in this paper let us quantify river SWS using a measurement based approach, providing new ability to constrain global storage dynamics. There are multiple long-term water surface elevation (Calmant et al., 2008; Coss et al., 2020; Tourian et al., 2016) and river surface water extent and width (Allen & Pavelsky, 2018; Huang et al., 2012; Yamazaki et al., 2015) datasets, including validated accuracy. Change in river storage can

be estimated directly from water surface elevation (WSE) and river width, as is routinely done with lake storage (Gao et al., 2012). While it is essentially impossible to directly validate CWS at the scale in our dataset, the uncertainty can be easily estimated based on the accuracy of WSE and width.

Here, we present the first published data product of volumetric river channel water storage anomaly (volumetric CWS) over 26 of the world's largest rivers using remotely sensed river WSEs and widths in the Global River Radar Altimetry Time Series 1 Kilometer Daily (GRRATS1kd, Coss et al., 2019a). We compute volumetric CWS directly from observations, and include analytical uncertainty estimates, allowing independent comparison with estimates based on hydrological modeling. In the context of volumetric CWS we define "anomaly" as the difference between a value at a particular time, and some reference time, t (e.g. the first date in our dataset). Storage change is the time derivative of storage, and can be calculated from the time derivative of the storage anomaly. GRACE TWS is also either a storage anomaly or storage change estimate; in this paper we use "TWS" to refer to storage anomaly. We use the new GRRATS1kd dataset to address three questions: 1) How large are storage variations within river mainstems compared to basin storage variations estimated by GRACE? We hypothesize that rivers are frequently hotspots of water storage variability, a part of watersheds where much greater water storage change tends to occur than elsewhere, since major rivers typically exhibit seasonal water level variation measuring several meters, while GRACE TWS seasonal changes are usually $<$ 500 mm across the entire basin (Felfelani et al., 2017; Humphrey & Gudmundsson, 2019). 2) What controls spatial patterns of storage variations in rivers? We hypothesize that patterns in storage variations will be controlled by river width and changes in drainage area at the location of tributary junctions. 3) How do estimates of river storage variations compare to modeled values? CWS can diagnose limitations in the meteorological forcing data, and provided input for assimilating measurement-based CWS (Emery et al., 2018; Getirana, Kumar, et al., 2017; Yamazaki et al., 2011). This is to our knowledge the first time modeled estimates of CWS have been evaluated using CWS values derived from measurements, and we expect the comparison to shed light on possible areas for models to improve. It is our hope that this this work can help to lay the ground work for further study of global surface water storage, as our ability to measure these is rapidly improving with each new satellite mission.

2 Methods and Datasets

GRRATS1kd is a one kilometer, one day resolution interpolated dataset spanning 26 of the world's largest rivers (Coss et al., 2019a); a list of the rivers is given in Table 1. GRRATS1kd comprises satellite altimetry measurements of river WSE interpolated to 1 km daily resolution, and volumetric CWS estimates computed from interpolated WSE and width. The virtual station data GRRATS (Coss et al., 2019b), is further described in (Coss et al., 2020). In this section, we briefly describe the datasets and major steps used to compute volumetric CWS.

The primary inputs to GRRATS1kd are measurements of river WSE at the intersection of radar altimeter ground tracks and rivers, or virtual stations (VS) (GRRATS, described by (Coss et al., 2020)), and river width measurements obtained using RivWidthCloud, a Landsat processing algorithm for measuring river width based on Google Earth Engine (Yang et al., 2019).

We analyzed data from two global SWS datasets. Both the Hydrological Modeling and Analysis Platform (Getirana et al., 2012; Getirana, Peters-Lidard, et al., 2017) and the Catchment-based Macro-scale Floodplain model (Yamazaki et al., 2011; 2014) are river routing schemes capable of simulating river and floodplain dynamics. Because it is not possible to validate CWS in our study, the inclusion of uncertainty is critical. Our uncertainty calculations are described in depth in (S2).

Below, we present three separate analyses of climatologies constructed from our data. Note that though this requires crossing confluences, their complexities have a minimal impact on storage change at this scale. First we compare with GRACE long-term average TWS climatology from the Center for Space Research at the University of Texas at Austin (http://www2.csr.utexas.edu/grace). See (S1) for details. For each basin, we create a 26 year volumetric CWS climatology summed over the length of the river (Figure 2B). We then find the amplitude of volumetric CWS climatology . Some analyses below present CA normalized by basin drainage area (i.e. we divide the CA value by the basin drainage area); we refer to this quantity as channel water storage (CWS) following the definition for GRACE TWS, CWS is presented with units of mm, and is comparable to GRACE.

Figure 1 for example, shows the Mississippi CA of 7.51 km^3 while the drainage area is 3,244,506 km^2. Dividing CA by drainage area results in a CWS of ~2.3mm.

In our discussion of the relationship of CWS to GRACE we reference mean slope data from (Coss et al., 2019b, 2020) and calculate an aridity index from net radiation from Clouds and the Earth's Radiant Energy System (CERES; Loeb et al., 2018; Wielicki et al., 1996) and Global Precipitation Climatology Project (GPCP; Adler et al., 2003).

Second, we relate CA, mean river width, and basin area at 1km resolution and test if different basin area groups have different CA/width relationships. To compare CA regimes, we relate our CA data to basin drainage area from Frasson et al., (2019) testing group regression lines for having statistically different slopes (S1). Third, we compare with global models by scaling the GRRATS1kd data up to the model grid resolution (1 or 0.1 degrees), by summing all our 1 km volumetric CWS data points that fall within each model grid cell. We then examine two criteria: 1) The CA for all cells overlapping our coverage channel; 2) Correlation coefficient of each model cell, with the average estimated CA from those estimated sections that fell within the cell. A more in depth description of methods is available in supplemental material (S1).

3 Results and Discussion

3.1 Uncertainty propagation

As direct validation of CWS is impossible, we have calculated uncertainty estimates for our volumetric CWS time series and the resulting climatologies. Mean volumetric CWS time series uncertainty ranges from 0.15 km^3 to 7.78 km^3 (on the Zambezi and Amazon rivers, respectively) with a median value 1.48 km^3. The mean volumetric CWS climatology uncertainty ranges from 0.03 km^3 to 1.54km^3 (on the Zambezi and Amazon rivers, respectively) with a median 0.3 km^3. Additionally, we calculated the maximum impact of uncertainty on CA and report it here as a ratio of uncertainty: CA. This value is calculated as the absolute difference between the maximum and minimum climatology within the uncertainty range, divided by the state CA. This value ranged from 0.09-2 (median 0.18). Four rivers had uncertainty that could account for >70% variation in CA (the Columbia, Parana, Sao Francisco, and Zambezi). While small CAs (<1km^3) might contribute to this high uncertainty in height: width fits used to generate changes in cross sectional area for times without data is the most likely. Input data (particularly widths) were limited in those basins. Just 1 river had uncertainty: CA of 2 (Sao Francisco) meaning some model results that were 2x greater than our CA estimates could be realistic. We find that the difference between model outputs and our estimates typically exceeds the disparity between our CWS estimates and their uncertainty.

3.2 The magnitude of main stem CWS as it relates to GRACE TWS

CWS ranges from 0.1 mm to 21.5 mm (on the Zambezi and Ayeyarwada rivers, respectively), with a mean value of 5.61 mm (Figure 2) on the 26 study rivers. As expected, the largest values are primarily from tropical basins. Table 1 shows the ratio of CWS compared with GRACE TWS (CWS:TWS ratio hereafter) climatology data constructed from Save et al. (2016) for each of the study river basins. Note that for GRACE comparison the Ganges and Brahmaputra basins have been combined. CWS:TWS ratio ranges from 0.04% to 12.53% (on the Zambezi and Uruguay Rivers respectively), with an average of 3.44 % of GRACE basin TWS. Surprisingly CWS contributes several percent of basin storage variability on average, despite mainstems representing an average of just 0.2% of total basin area (Table 1). This analysis highlights rivers as storage hotspots, parts of major drainage basins where an oversized fraction of storage variation takes place.

CWS: TWS varies over two orders of magnitude on Study Rivers, evincing tremendous diversity across global basins in rivers' role in overall basin storage. As the mainstem combines both upstream hydrologic processes and river hydraulics, we explored the role of basin aridity index (long-term average potential evaporation to precipitation; see (McMahon et al., 2013)) and mainstem slope in the CWS:TWS. We hypothesized that basins with high AI would have a lower total runoff, and a lower CWS: TWS ratio, and that basins with low slope would have slower flow velocities, longer channel residence times, and larger

CWS: TWS ratios. Ultimately we found that the percentage of the basin measured (not slope or AI) does have some impact on CWS: TWS ratio ($R^2 = 0.58$), but this finding heavily impacted by an outlier ($R^2 = 0.24$, without Uruguay). It unclear what factors drive this variability though CWS coverage area is a factor. A more in depth analysis of this work is available in the supplement (TS4,FS1:3).

3.3 volumetric CWS climatology amplitude regimes

While we might expect volumetric CWS climatology amplitude (CA) to increase monotonically with distance downstream, this was frequently not the case (Rodríguez-Iturbe et al., 1992). We sometimes see the opposite (Congo, Figure 2) , and most frequently find that CA hotspots occur in a variety of locations on the mainstem of a river (Amazon, Mississippi). Controls on spatial patterns of CA in rivers are diverse and complex. The Amazon, for example, has large flood plain lakes that suppress surface elevation variation (Bonnet et al., 2008). In an effort to quantify this phenomenon, we compare the relationship between CA and mean channel width, and basin drainage area at 1 km resolution for 19 of the rivers for which drainage area data are available from Frasson et al. (2019). Generally, as width increases, the CA increases as well (Figure 3). This is not a uniformly applicable principle, however. Relative Amplitude (e.g. Figure 1a) does not increase uniformly in all rivers as they widen downstream. This means consideration of variation in space is critical for understanding individual rivers' volumetric CWS signature. However, most rivers show distinct relationships that can be explained by drainage area. Because of the river sections being analyzed, only 15 of the 19 rivers can be subdivided into 2 or more distinguishable (drainage area difference $> 10\%$) groups. For these 15 rivers, all but 2 show the expected relationship between CA, mean width, and drainage area (Amur and Brahmaputra) where the slope of the CA : width relationship changes significantly with drainage area. Full results are available in supplemental material (Figure S4 and Table S3). For the Amur and Brahmaputra rivers, the slope change is not statistically significant (magnitude of $Z<2$). Despite large variation in local storage magnitudes at the 1km scale, the general trend of changing CA, mean width, and drainage area holds at the river scale.

3.4 Model Comparisons

While comparison of GRRATS1kd with HyMAP and CaMa-flood reveals promising similarity between model and estimate data on some rivers (Figure 4), HyMAP and CaMa-flood reasonably approximate CA in 30.7% and 11.5% of the rivers respectively. We define "reasonable" as having a climatology amplitude within $\pm 50\%$ (Wrzesien et al., 2017). We show the cumulative distribution function of these amplitude comparisons for all rivers in Figure 4D (amplitude ratios<4) to provide a more comprehensive view of these data. With few exceptions, model and our estimates are generally in phase; Figure 4c is an exception. To assess the capabilities of the models to represent spatial patterns in CA, we also compared the Spatial normalized CA, that is the spatial series of our es-

timates and modeled climatology amplitude, after gridding GRRATS1kd onto the model grid. Generally, we found that the models represent the seasonal amplitude better than spatial patterns. At the grid cell level, we compared seasonal amplitude from the models and our estimates. For CaMa-flood we find that 65% of rivers (42% statistically significant) have an average cell correlation >0 (15.3% >0.5), with a maximum value of 0.9. HyMAP results show 65.4% of rivers (11.5% statistically significant) with an average cell correlation >0 (15% >0.5), with a maximum value of 0.91. Overall, these results demonstrate that while models often represent the magnitude of this signal well, they often misrepresent the location of the water. Variation in scaling and model precipitation inputs could contribute many of the differences we see between the models and our estimate values. When we looked at the modeled volumetric CWS components (width and height variation) in greater depth we found that the standard deviation of height often exceeds our estimates (median value of 70.3% and 99.6% of cells in HyMap and CaMa-Flood respectively). Details can be found in supplemental material (table S3). It is possible that overestimation of height variation and simplified width variation heavily impact where this variation happens in the models.

5 Conclusions

Here we use a new remote sensing dataset (volumetric CWS) to explore the role of major world rivers in the global water cycle. We find that rivers are storage hotspots, parts of major drainage basins with exceptionally large fractions of total storage variation. Specifically, by comparing our dataset with GRACE, we showed that the mainstem river accounted for a highly variable percentage (0.04%-12.54%) of TWS variation within the basin, for study rivers. We hypothesize an array of complex factors, including basin hydrology and river hydraulics, govern the ratio of river to TWS change among basins; our preliminary results show that basin-averaged aridity index and river slope do not explain these variations, though coverage area is an important factor (24% correlation).

We find that within-river spatial patterns in channel water storage climatology anomaly are highly complex, and do not simply increase monotonically with distance downstream as we hypothesized. Frequently the opposite pattern emerges, though highly variable patterns in CWS are most common. We find that the width and channel water storage climatology relationship generally changes with flow accumulation (expected behavior), though two study rivers did not show this. Third, we find study models capture the amplitude of river storage variations more successfully than they represent river water storage spatially. We find HyMap and CaMa-Flood represent CWS climatology amplitude reasonably ($\pm$50%) in only 30.7% and 11.5% of rivers considered respectively. We also find that HyMap and CaMa-Flood cells significantly correlate spatially with our estimate data on just 42% and 11.5% of rivers respectively. We did not diagnose the cause of these discrepancies but hypothesize that anthropogenic management (not simulated) play an important role. Future work should explore assimilation of channel water storage into such models, as well as integration with

existing datasets measuring floodplains and reservoirs. Such work is even more important given recent and future datasets that represent improved height and inundated area measurements from sensors such as Planet, Sentinel -2, Landsat 8+9 and the upcoming SWOT mission (Boshuizen et al., 2014; Drusch et al., 2012; Fu et al., 2009; Markham et al., 2019; Roy et al., 2014). As Durand et al., (2021) suggests, the ever growing constellation of remote sensing platforms brings us closer and close to being able to quantify surface water processes globally and a multisensor data, multidisciplinary approach is an important aspect for progress in the field of global hydrology.

Acknowledgments and Data

The authors report no conflicts of interest.

The data used in this study (DOI: 10.5067/PSGRA-DA2V2) is available on the NASA PO.DAAC (https://podaac.jpl.nasa.gov/dataset/PRESWOT_HYDRO_GRRATS_L2_DAILY_VIRTUAL_STATION_HEIGHTS_V2?ids=&values=).

This work was supported by a NASA FINESST award (GRT00054946).

References

Adler, R. F., Huffman, G. J., Chang, A., Ferraro, R., Xie, P.-P., Janowiak, J., et al. (2003). The version-2 global precipitation climatology project (GPCP) monthly precipitation analysis (1979-present). *Journal of Hydrometeorology*, *4*(6), 1147–1167.Allen, G. H., & Pavelsky, T. M. (2018). Global extent of rivers and streams. *Science*, *361*(6402), 585. https://doi.org/10.1126/science.aat0636Bonnet, M. P., Barroux, G., Martinez, J. M., Seyler, F., Moreira-Turcq, P., Cochonneau, G., et al. (2008). Floodplain hydrology in an Amazon floodplain lake (Lago Grande de Curuaí). *Journal of Hydrology*, *349*(1), 18–30. https://doi.org/10.1016/j.jhydrol.2007.10.055Boshuizen, C., Mason, J., Klupar, P., & Spanhake, S. (2014). Results from the planet labs flock constellation.Calmant, S., Seyler, F., & Cretaux, J. F. (2008). Monitoring continental surface waters by satellite altimetry. *Surveys in Geophysics*, *29*(4–5), 247–269.Coss, S., Durand, M., Lettenmaier, D., Yi, Y., Jia, Y., Guo, Q., et al. (2019a). Pre SWOT Hydrology GRRATS Daily River Heights and Storage Version 2. *PO.DAAC*. https://doi.org/10.5067/PSGRA-DA2V2Coss, S., Durand, M., Lettenmaier, D., Yi, Y., Jia, Y., Guo, Q., et al. (2019b). Pre SWOT Hydrology GRRATS Virtual Station River Heights Version 2. NASA Physical Oceanography DAAC. https://doi.org/10.5067/PSGRA-SA2V2Coss, S., Durand, M., Yi, Y., Jia, Y., Guo, Q., Tuozzolo, S., et al. (2020). Global River Radar Altimetry Time Series (GRRATS): new river elevation earth science data records for the hydrologic community. *Earth Syst. Sci. Data*, *12*(1), 137–150. https://doi.org/10.5194/essd-12-137-2020Döll, P., Hoffmann-Dobrev, H., Portmann, F. T., Siebert, S., Eicker, A., Rodell, M., et al. (2012). Impact of water withdrawals from groundwater and surface water on continental water storage variations. *Journal of Geodynamics*, *59–60*, 143–156. https://doi.org/10.1016/j.jog.2011.05.001Drusch, M., Del Bello, U.,

Carlier, S., Colin, O., Fernandez, V., Gascon, F., et al. (2012). Sentinel-2: ESA's optical high-resolution mission for GMES operational services. *Remote Sensing of Environment*, *120*, 25–36.Durand, M., Barros, A., Dozier, J., Adler, R., Cooley, S., Entekhabi, D., et al. (2021). Achieving Breakthroughs in Global Hydrologic Science by Unlocking the Power of Multisensor, Multidisciplinary Earth Observations. *AGU Advances*, *2*(4), e2021AV000455. https://doi.org/10.1029/2021AV000455Emery, C. M., Paris, A., Biancamaria, S., Boone, A., Calmant, S., Garambois, P.-A., & da Silva, J. S. (2018). Large-scale hydrological model river storage and discharge correction using a satellite altimetry-based discharge product. *Hydrology and Earth System Sciences*, *22*(4), 2135.Famiglietti, J., Cazenave, A., Eicker, A., Reager, J., Rodell, M., & Velicogna, I. (2015). Satellites provide the big picture. *Science (New York, NY)*, *349*(6249), 684–685.Felfelani, F., Wada, Y., Longuevergne, L., & Pokhrel, Y. N. (2017). Natural and human-induced terrestrial water storage change: A global analysis using hydrological models and GRACE. *Journal of Hydrology*, *553*, 105–118. https://doi.org/10.1016/j.jhydrol.2017.07.048Frasson, R. P. de M., Pavelsky, T. M., Fonstad, M. A., Durand, M. T., Allen, G. H., Schumann, G., et al. (2019). Global relationships between river width, slope, catchment area, meander wavelength, sinuosity, and discharge. *Geophysical Research Letters*, *46*(6), 3252–3262.Fu, L.-L., Alsdorf, D., Rodriguez, E., Morrow, R., Mognard, N., Lambin, J., et al. (2009). The SWOT (Surface Water and Ocean Topography) mission: spaceborne radar interferometry for oceanographic and hydrological applications. Presented at the OCEANOBS'09 Conference, Citeseer.Gao, H., Birkett, C., & Lettenmaier, D. P. (2012). Global monitoring of large reservoir storage from satellite remote sensing. *Water Resources Research*, *48*(9). https://doi.org/10.1029/2012WR012063Getirana, A., Boone, A., Yamazaki, D., Decharme, B., Papa, F., & Mognard, N. (2012). The hydrological modeling and analysis platform (HyMAP): Evaluation in the Amazon basin. *Journal of Hydrometeorology*, *13*(6), 1641–1665.Getirana, A., Kumar, S., Girotto, M., & Rodell, M. (2017). Rivers and Floodplains as Key Components of Global Terrestrial Water Storage Variability. *Geophysical Research Letters*, *44*(20), 10,359-10,368. https://doi.org/10.1002/2017GL074684Getirana, A., Peters-Lidard, C., Rodell, M., & Bates, P. D. (2017). Trade-off between cost and accuracy in large-scale surface water dynamic modeling. *Water Resources Research*, *53*(6), 4942–4955. https://doi.org/10.1002/2017WR020519Huang, S., Li, J., & Xu, M. (2012). Water surface variations monitoring and flood hazard analysis in Dongting Lake area using long-term Terra/MODIS data time series. *Natural Hazards*, *62*(1), 93–100. https://doi.org/10.1007/s11069-011-9921-6Humphrey, V., & Gudmundsson, L. (2019). GRACE-REC: a reconstruction of climate-driven water storage changes over the last century. *Earth System Science Data*, *11*(3), 1153–1170. https://doi.org/10.5194/essd-11-1153-2019Lettenmaier, D. P., Alsdorf, D., Dozier, J., Huffman, G. J., Pan, M., & Wood, E. F. (2015). Inroads of remote sensing into hydrologic science during the WRR era. *Water Resources Research*, *51*(9), 7309–7342.Llovel, W., Becker, M., Cazenave, A., Crétaux, J.-F., & Ramillien, G. (2010). Global land water storage change from GRACE over 2002–2009; Inference on sea level.

Comptes Rendus Geoscience, *342*(3), 179–188.Loeb, N. G., Su, W., Doelling, D. R., Wong, T., Minnis, P., Thomas, S., & Miller, W. F. (2018). 5.03 - Earth's Top-of-Atmosphere Radiation Budget. In S. Liang (Ed.), *Comprehensive Remote Sensing* (pp. 67–84). Oxford: Elsevier. https://doi.org/10.1016/B978-0-12-409548-9.10367-7MarkhamM, B., Barsi, J., Donley, E., Efremova, B., Hair, J., Jenstrom, D., et al. (2019). Landsat 9: Mission status and prelaunch instrument performance characterization and calibration (pp. 5788–5791). Presented at the IGARSS 2019-2019 IEEE International Geoscience and Remote Sensing Symposium, IEEE.McMahon, T., Laaha, G., Parajka, J., Peel, M., Savenije, H., Sivapalan, M., et al. (2013). Prediction of annual runoff in ungauged basins.Oki, T., & Kanae, S. (2006). Global hydrological cycles and world water resources. *Science*, *313*(5790), 1068–1072.Papa, F., Frappart, F., Güntner, A., Prigent, C., Aires, F., Getirana, A. C. V., & Maurer, R. (2013). Surface freshwater storage and variability in the Amazon basin from multi-satellite observations, 1993–2007. *Journal of Geophysical Research: Atmospheres*, *118*(21), 11,951-11,965. https://doi.org/10.1002/2013JD020500Papa, F., Frappart, F., Malbeteau, Y., Shamsudduha, M., Vuruputur, V., Sekhar, M., et al. (2015). Satellite-derived surface and sub-surface water storage in the Ganges–Brahmaputra River Basin. *Groundwater Systems of the Indian Sub-Continent*, *4*, 15–35. https://doi.org/10.1016/j.ejrh.2015.03.004Rodell, M., Famiglietti, J. S., Wiese, D. N., Reager, J. T., Beaudoing, H. K., Landerer, F. W., & Lo, M.-H. (2018). Emerging trends in global freshwater availability. *Nature*, *557*(7707), 651–659. https://doi.org/10.1038/s41586-018-0123-1Rodríguez-Iturbe, I., Ijjász-Vásquez, E. J., Bras, R. L., & Tarboton, D. G. (1992). Power law distributions of discharge mass and energy in river basins. *Water Resources Research*, *28*(4), 1089–1093. https://doi.org/10.1029/91WR03033Roy, D. P., Wulder, M. A., Loveland, T. R., Woodcock, C., Allen, R. G., Anderson, M. C., et al. (2014). Landsat-8: Science and product vision for terrestrial global change research. *Remote Sensing of Environment*, *145*, 154–172.Swenson, S., Famiglietti, J., Basara, J., & Wahr, J. (2008). Estimating profile soil moisture and groundwater variations using GRACE and Oklahoma Mesonet soil moisture data. *Water Resources Research*, *44*(1).Syed, T. H., Famiglietti, J. S., Rodell, M., Chen, J., & Wilson, C. R. (2008). Analysis of terrestrial water storage changes from GRACE and GLDAS. *Water Resources Research*, *44*(2).Tapley, B. D., Bettadpur, S., Watkins, M., & Reigber, C. (2004). The gravity recovery and climate experiment: Mission overview and early results. *Geophysical Research Letters*, *31*(9).Tapley, B. D., Watkins, M. M., Flechtner, F., Reigber, C., Bettadpur, S., Rodell, M., et al. (2019). Contributions of GRACE to understanding climate change. *Nature Climate Change*, *9*(5), 358–369.Tortini, R., Noujdina, N., Yeo, S., Ricko, M., Birkett, C. M., Khandelwal, A., et al. (2020). Satellite-based remote sensing data set of global surface water storage change from 1992 to 2018. *Earth System Science Data*, *12*(2), 1141–1151. https://doi.org/10.5194/essd-12-1141-2020Tourian, M., Tarpanelli, A., Elmi, O., Qin, T., Brocca, L., Moramarco, T., & Sneeuw, N. (2016). Spatiotemporal densification of river water level time series by multimission satellite altimetry. *Water Resources Research*.Wielicki, B.

A., Barkstrom, B. R., Harrison, E. F., Lee, R. B., III, Smith, G. L., & Cooper, J. E. (1996). Clouds and the Earth's Radiant Energy System (CERES): An Earth Observing System Experiment. *Bulletin of the American Meteorological Society*, *77*(5), 853–868. https://doi.org/10.1175/1520-0477(1996)077<0853:CATERE>2.0.CO;2Wrzesien, M. L., Durand, M. T., Pavelsky, T. M., Howat, I. M., Margulis, S. A., & Huning, L. S. (2017). Comparison of methods to estimate snow water equivalent at the mountain range scale: a case study of the California Sierra Nevada. *Journal of Hydrometeorology*, *18*(4), 1101–1119.Yamazaki, D., Kanae, S., Kim, H., & Oki, T. (2011). A physically based description of floodplain inundation dynamics in a global river routing model. *Water Resources Research*, *47*(4). https://doi.org/10.1029/2010WR009726Yamazaki, D., Sato, T., Kanae, S., Hirabayashi, Y., & Bates, P. D. (2014). Regional flood dynamics in a bifurcating mega delta simulated in a global river model. *Geophysical Research Letters*, *41*(9), 3127–3135. https://doi.org/10.1002/2014GL059744Yamazaki, D., Trigg, M. A., & Ikeshima, D. (2015). Development of a global ~ 90 m water body map using multi-temporal Landsat images. *Remote Sensing of Environment*, *171*, 337–351. https://doi.org/10.1016/j.rse.2015.10.014Yang, X., T. M. Pavelsky, G. H. Allen, & G. Donchyts. (2019). RivWidthCloud: An Automated Google Earth Engine Algorithm for River Width Extraction From Remotely Sensed Imagery. *IEEE Geoscience and Remote Sensing Letters*, 1–5. https://doi.org/10.1109/LGRS.2019.2920225

Figure 1.

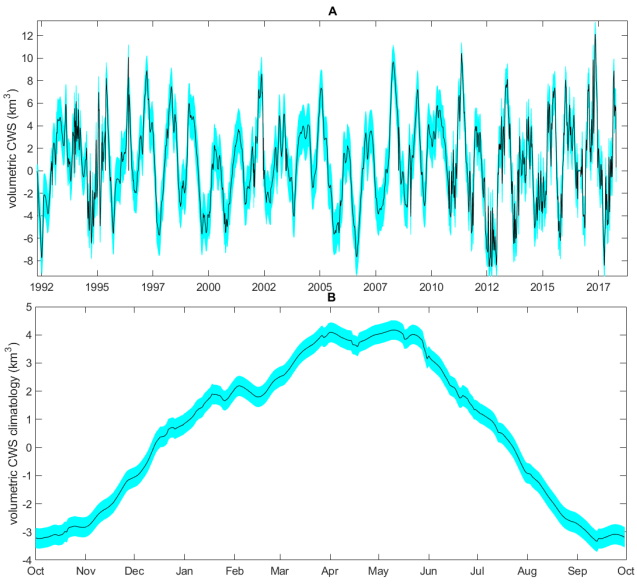

Figure 1. Mississippi volumetric CWS time series. Panel A is the complete record, while panel B shows constructed climatology (volumetric CWS climatol-

ogy). In both panels, uncertainty is shown with blue error bars. The Mississippi climatology amplitude (CA) is 7.51 km^3 while the drainage area is 3,244,506 km^2. Dividing CA by drainage area results in a CWS of ~2.3mm.

Figure 2.

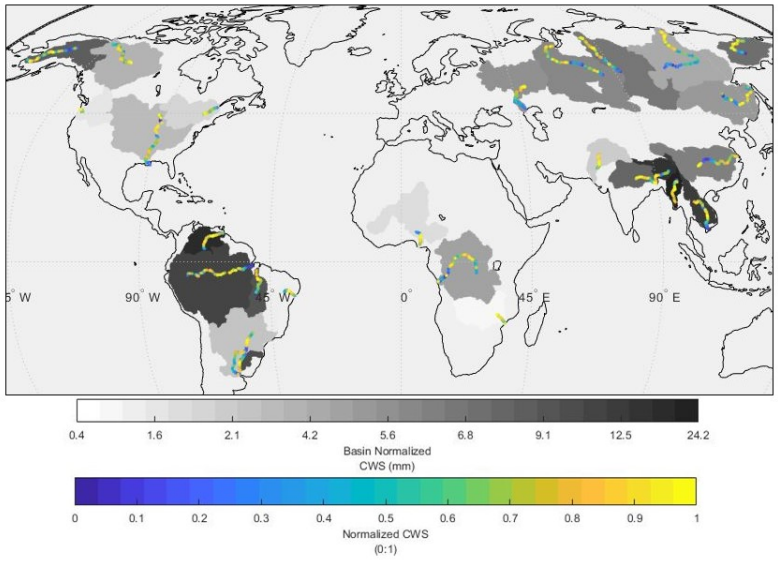

Figure 2. CWS (basin normalized CA in mm) shown in greyscale. Individual 1km CA segment data shown in blue-yellow color scale rescaled between zero and 1 (following formula S1) to highlight where rivers store their water. Every 100th point shown.

Figure 3.

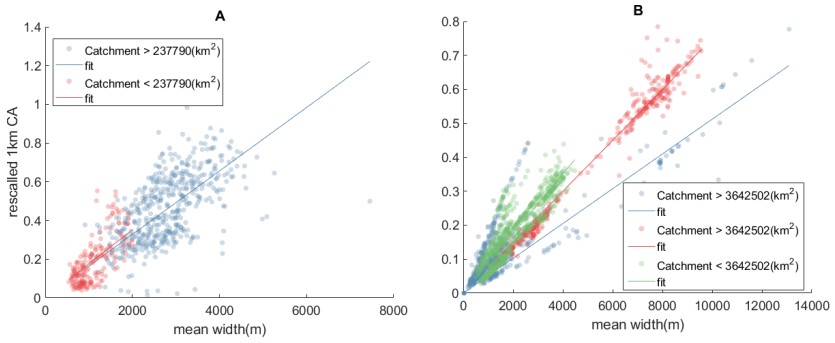

Figure 3. 1 km section CA (as seen in Figure 2 river lines) and mean width plots for the Amur (A), and Congo (B) basins. Data is plotted by drainage area and fit with a least squares regression line per catchment regime. Data is grouped by large increases in in flow accumulation to avoid comparison across large tributaries. We then re-assimilated any divisions that did not achieve a change in basin drainage area>10 %.

Figure 4.

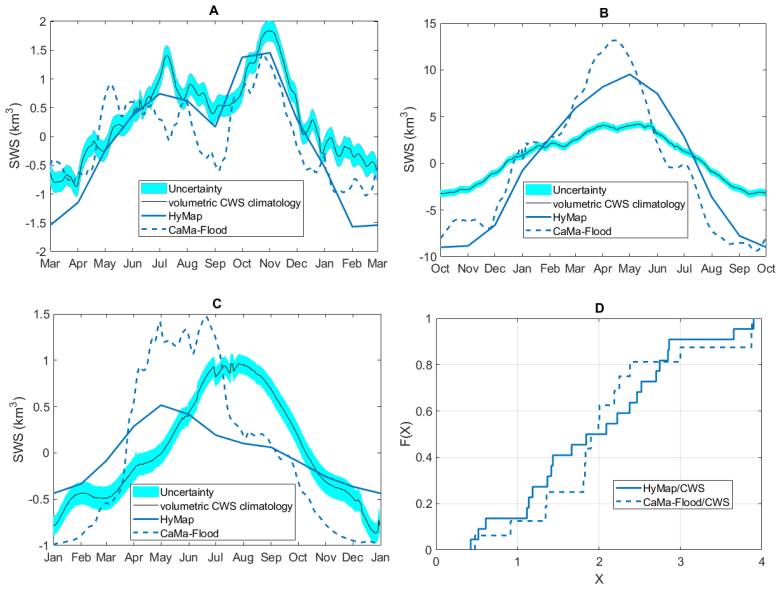

Figure 4 Storage change climatology plots for the Uruguay (A), Mississippi (B), and Indus (C) Rivers. HyMAP data is shown in solid blue, CaMa-flood is shown in dashed blue, and volumetric CWS climatology is shown in in black, and its uncertainty is plotted in light blue. Panel D shows the CDF of amplitude ratio comparisons from both models (amplitude ratios<4).

Table 1.

Table 1 Percentage of GRACE TWS estimated in mainstem CWS, basin drainage areas, CWS coverage area, inundated area from GRWL, and CA regime change.

River	**% GRACE TWS**	**Basin drainage area (km^2)**	**CWS coverage area (km^2)**	**GRWL inundated area (km^2)**	**1km CA/ Width slope change with drainage area**
Amazon		,888,268	,702	,673	Yes
Amur		,101,598	,808	,194	no
Ayeyarwada		,438	,449	,199	Yes
Columbia		,035		,543	Yes
Congo		,689,187	,362	,813	Yes
Ganges-Brahmaputra		,792,035	,293	,160	no
Indus		,062		,330	-
Kolyma		,254	,928	,150	-
Lena		,467,695	,507	,836	-
Mackenzie		,805,884	,559	,749	-
Mekong		,231	,244	,197	Yes
Mississippi		,244,506	,709	,002	Yes
Niger		,115,246		,019	-
Ob		,929,051	,757	,176	-
Orinoco		,352	,899	,537	Yes
Parana		,639,954	,096	,843	Yes
SaoFrancisco		,842	,132	,088	Yes
St Lawrence		,055,756	,531	,606	-
Tocantins		,445	,000	,914	-
Uruguay		,786	,872	,183	Yes
Volga		,410,756	,787	,857	-
Yangtze		,908,837	,460	,550	Yes
Yenisei		,518,211	,305	,558	-
Yukon		,373,188	,067	,687	-
Zambezi		,373,188		,186	No